Received: 13 October 2023 | Revised: 30 November 2023 | Accepted: 12 December 2023

DOI: 10.1002/pro.4872

RESEARCH ARTICLE

THE PROTEIN SOCIETY WILEY

Helicity of a tardigrade disordered protein contributes to its protective function during desiccation

Sourav Biswas[1] | **Edith Gollub**[2,3] | **Feng Yu**[2,3] | **Garrett Ginell**[4,5] | **Alex Holehouse**[4,5] | **Shahar Sukenik**[2,3] | **Thomas C. Boothby**[1]

[1]Department of Molecular Biology, University of Wyoming, Laramie, Wyoming, USA

[2]Department of Chemistry and Biochemistry, University of California, Merced, Merced, California, USA

[3]Quantitative Systems Biology Program, University of California Merced, Merced, California, USA

[4]Department of Biochemistry and Molecular Biophysics, Washington University School of Medicine, St. Louis, Missouri, USA

[5]Center for Biomolecular Condensates, Washington University in St. Louis, St. Louis, Missouri, USA

Correspondence
Thomas C. Boothby, Department of Molecular Biology, University of Wyoming, Dept 4325, Science Initiative Building, 1000 E. University Ave, Laramie, WY 82071, USA.
Email: tboothby@uwyo.edu

Funding information
National Science Foundation, Grant/Award Numbers: 2128068, 2128067, 2128069, 2213983; Wyoming NASA EPSCoR, Grant/Award Number: #80NSSC19M0061; USDA National Institute of Food and Agriculture, Grant/Award Number: #1012152

Review Editor: Aitziber L. Cortajarena

Abstract

To survive extreme drying (anhydrobiosis), many organisms, spanning every kingdom of life, accumulate intrinsically disordered proteins (IDPs). For decades, the ability of anhydrobiosis-related IDPs to form transient amphipathic helices has been suggested to be important for promoting desiccation tolerance. However, evidence empirically supporting the necessity and/or sufficiency of helicity in mediating anhydrobiosis is lacking. Here, we demonstrate that the linker region of CAHS D, a desiccation-related IDP from the tardigrade *Hypsibius exemplaris*, that contains significant helical structure, is the protective portion of this protein. Perturbing the sequence composition and grammar of the linker region of CAHS D, through the insertion of helix-breaking prolines, modulating the identity of charged residues, or replacement of hydrophobic amino acids with serine or glycine residues results in variants with different degrees of helical structure. Importantly, correlation of protective capacity and helical content in variants generated through different helix perturbing modalities does not show as strong a trend, suggesting that while helicity is important, it is not the only property that makes a protein protective during desiccation. These results provide direct evidence for the decades-old theory that helicity of desiccation-related IDPs is linked to their anhydrobiotic capacity.

KEYWORDS

anhydrobiosis, CAHS, dehydration, desiccation tolerance, disordered protein, helicity, tardigrade

1 | INTRODUCTION

Water is required for all metabolism, so the adage "water is life" is commonly used to imply that without water, life cannot persist (Armstrong & Johnson, 2018). However, diverse organisms, spanning every kingdom of life, contradict this statement through their ability to enter into a drying-induced state of suspended animation known as anhydrobiosis (life without water) (Tunnacliffe & Lapinski, 2003). In this anhydrobiotic state, these organisms can persist for years, decades, or in the case of some ancient seeds, even millennia, but resume metabolism and

life processes upon rehydration (Crowe et al., 1992; Crowe & Clegg, 1973; Sallon et al., 2008).

Decades of work have identified non-reducing disaccharides, such as trehalose, as major molecular mediators that promote anhydrobiosis in a number of organisms (Crowe et al., 1984; Erkut et al., 2011; Tapia & Koshland, 2014). However, more recent work has demonstrated that some organisms that robustly survive desiccation, such as tardigrades and bdelloid rotifers, produce low or undetectable levels of trehalose (Boothby & Pielak, 2017; Caprioli et al., 2004; Cesari et al., 2012; Hara et al., 2021; Hengherr et al., 2008; Jönsson & Persson, 2010; Lapinski & Tunnacliffe, 2003; Nguyen et al., 2022; Tunnacliffe et al., 2005; Westh & Ramløv, 1991). While these discoveries do not reduce the importance or necessity of trehalose, and other co-solutes, in mediating desiccation tolerance in some organisms, they do reveal that additional mediators likely play important roles in surviving extreme drying.

An emerging paradigm in the anhydrobiosis field is the involvement of intrinsically disordered proteins (IDPs) in mediating desiccation tolerance (Boothby et al., 2017; Boothby & Pielak, 2017; Romero-Perez et al., 2023; Tunnacliffe et al., 2010; Yamaguchi et al., 2012). Some of the first IDPs implicated in anhydrobiosis were late embryogenesis abundant (LEA) proteins, which were first identified in cotton seeds (Dure et al., 1981), but have subsequently been found in a number of diverse organisms (Battista et al., 2001; Browne et al., 2002; Dure et al., 1981; Hand et al., 2011; Kikawada et al., 2006; Schokraie et al., 2010; Tunnacliffe et al., 2005). Following their initial discovery, LEA proteins have been classified into seven distinct families, and other desiccation-related IDPs have been identified (Battaglia et al., 2008; Belott et al., 2020; Boothby et al., 2017; Dorone et al., 2021; Tanaka et al., 2015; Yamaguchi et al., 2012). These include LEA-like proteins or hydrophilins (Battaglia et al., 2008), which are typified by a predominance of hydrophilic residues (Garay-Arroyo et al., 2000), as well as three families of tardigrade disordered proteins (TDPs) termed cytoplasmic, mitochondrial, and secreted abundant heat soluble (CAHS, MAHS, and SAHS, respectively) proteins (Hesgrove & Boothby, 2020; Tanaka et al., 2015; Yamaguchi et al., 2012).

While IDPs lack a stable tertiary structure, this does not preclude them from adopting transient secondary structure (Habchi et al., 2014). Members of several LEA families, as well as CAHS, MAHS, and SAHS proteins, have been shown to possess transient helices and/or to take on additional helicity during drying and/or chemical desolvation (Bremer et al., 2017; Cuevas-Velazquez et al., 2016; Hand et al., 2011; Tanaka et al., 2015; Tolleter et al., 2010; Yamaguchi et al., 2012). Adoption of helical structure in these proteins often results in the appearance of amphipathicity, that is, the appearance of a hydrophobic and polar face (Hincha & Thalhammer, 2012; Yamaguchi et al., 2012). This phenomenon has been described in a myriad of studies, many of which propose that helicity of these proteins drives their protective capacity during anhydrobiosis (Cuevas-Velazquez et al., 2016; LeBlanc & Hand, 2021; Yamaguchi et al., 2012).

Although helicity has been proposed to play a role in desiccation protection, direct evidence testing this hypothesis is limited. One study identified a correlation between freeze tolerance and helicity in a cold-regulated LEA protein (Sowemimo et al., 2019). However, to our knowledge, no published work has directly tested the link between the helicity of a desiccation-related IDP and its ability to confer protection during drying.

Here, we directly test the necessity of the helicity of the tardigrade IDP, CAHS D, in protecting the labile enzyme lactate dehydrogenase (LDH) during desiccation. CAHS D is largely disordered, existing in an ensemble of states that resemble a dumbbell composed of two collapsed terminal regions held apart by an extended helical linker (Eicher et al., 2022; Malki et al., 2022; Sanchez-Martinez, Nguyen, et al., 2023). We find that the highly helical linker region of CAHS D promotes the protection of LDH. Furthermore, the tandem duplication of the linker flanked by endogenous N- and C-termini results in a variant with similar protective capacity relative to wild-type CAHS D. Replacement of the linker region with an exogenous sequence results in reduced helicity and a concomitant decrease in protection. Finer scale disruptions of the linker's helicity via charge identity swapping result in correlated decreases in protection as does the insertion of helix-breaking prolines or the replacement of hydrophobic residues with serine/glycine. In every variant that decreases helicity of CAHS D or its linker region, we observe a decrease in protective capacity. Furthermore, we find that the helicity of variants generated by a similar modality (e.g., insertion of prolines) correlates well with protective capacity. However, this correlation decreases when comparing variants generated through different modalities (e.g., insertion of prolines versus charged residues swapping), implying that helicity is mechanistically linked to desiccation protection in CAHS D, but is not the only factor governing this phenomenon.

2 | RESULTS

2.1 | CAHS D is a representative CAHS protein

To address the question of whether the helicity of desiccation-related IDPs is necessary for promoting their protective capacity during drying, we chose to study

CAHS proteins. This decision was made since these CAHS proteins are known to contain transient helical structure which increases upon desolvation (Yamaguchi et al., 2012), and they confer protection during drying (Boothby et al., 2017; Packebush et al., 2023; Piszkiewicz et al., 2019; Tanaka et al., 2022).

One of the best-characterized CAHS proteins is CAHS D, a representative CAHS protein from tardigrade *Hypsibius exemplaris*. CAHS D has been shown to be required for robust desiccation tolerance in tardigrades, to confer desiccation tolerance to labile enzymes in vitro, and to promote anhydrobiosis when exogenously expressed in yeast and bacteria (Boothby et al., 2017). Biophysical and computational studies have shown that CAHS D occupies a dumbbell-like ensemble of interconverting conformations composed of two relatively compact termini bridged by an internal linker region (Figure 1a) (Eicher et al., 2022; Malki et al., 2022; Sanchez-Martinez, Nguyen, et al., 2023). The terminal regions of CAHS D contain transient helical and

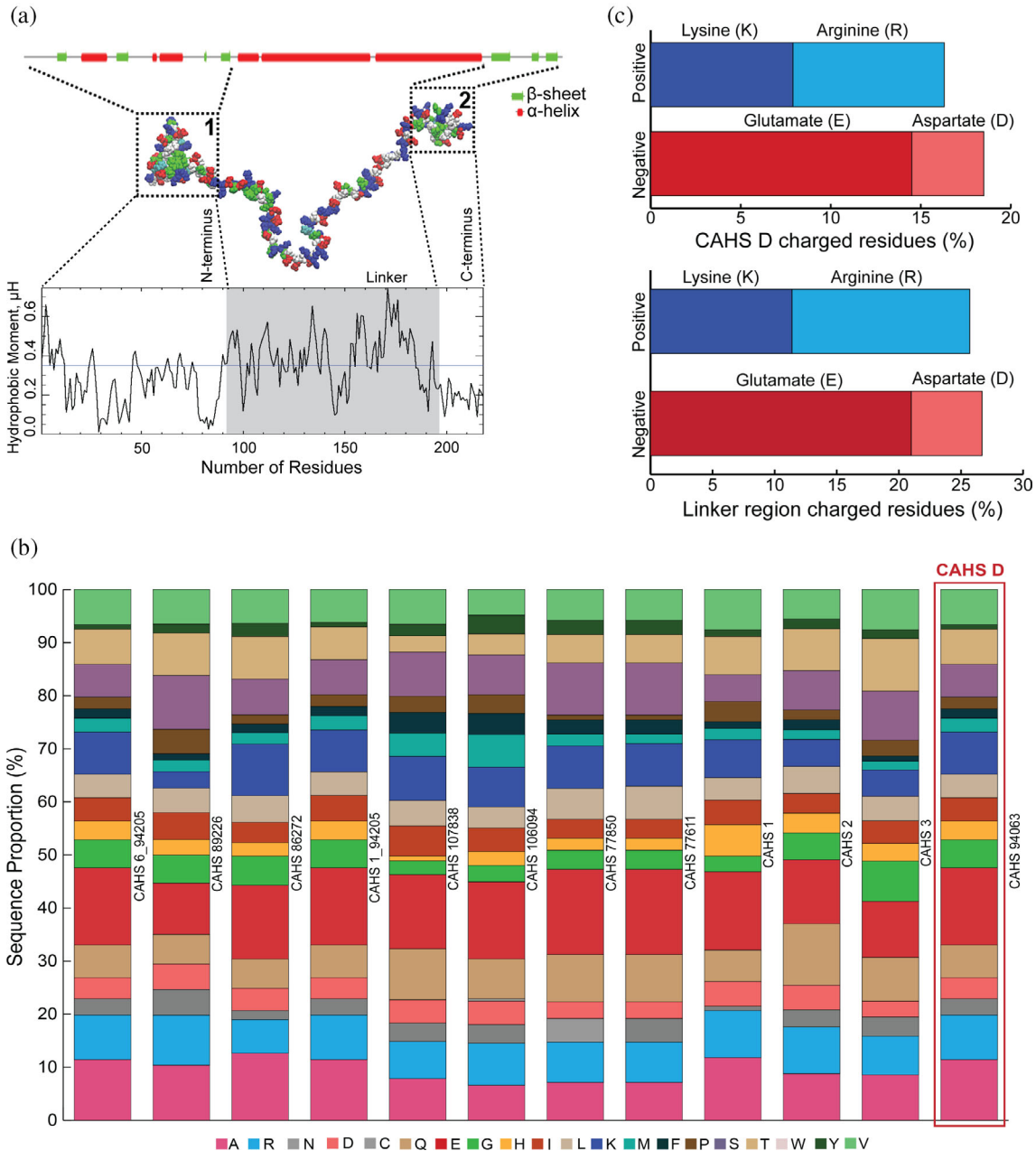

FIGURE 1 CAHS D, a model CAHS protein. (a) Representative conformational ensemble of model CAHS D protein by all-atom Monte Carlo simulation (Sanchez-Martinez, Nguyen, et al., 2023). Helix/sheet assignments made using JPRED4 (Drozdetskiy et al., 2015). CAHS D hydrophobic moment per amino acid residue calculated by EMBOSS Hydrophobic Moment Calculator (Eisenberg et al., 1982). (b) Amino acid composition of CAHS proteins. (c) Percentage of charged residues in full-length CAHS D (top) and the CAHS D linker region (bottom).

beta-structure, while the linker region interconverts between random coil and helical structures (Eicher et al., 2022; Malki et al., 2022; Sanchez-Martinez, Nguyen, et al., 2023) (Figure 1a). The CAHS linker contains both polar and hydrophobic residues, and when in a helical state, this region exists as an amphipathic helix, as quantified by the hydrophobic moment (Figure 1a).

Disordered proteins can be classified by sequence properties, including the fraction of charged residues (FCRs), net charge per residue (NCPR), and hydropathy (Das & Pappu, 2013). With this in mind, CAHS D resembles other CAHS proteins in the UniProt database (File S1) in terms of these and other properties, including FCR, NCPR, hydropathy, disorder content, protein length, and overall amino acid composition. CAHS proteins, including CAHS D, have high FCR (Figure 1b) and a low kappa (κ), a measure of charge distribution (Table 1). Beyond a high FCR, CAHS D is representative of other CAHS proteins in that an approximately equal proportion of positively charged amino acids; lysine (K) and arginine (R) are present, while there is a bias between negatively charged residues; more glutamate (E) as compared to aspartate (D) (Figure 1b,c). Furthermore, computational analysis (Metapredict and Alphafold2) shows that at the level of ensemble, CAHS D is predicted to resemble other CAHS proteins in the UniProt database, which are predicted to have helical structure in an internal region spanning amino acids ~91 to ~195 (Table 1). An exception to this is CAHS 89226, which is larger than other CAHS proteins (414 aa) and whose internal helical linker region is correspondingly offset (~280–380 aa) (Table 1). Thus, since CAHS D's sequence and ensemble features mirror those of other CAHS proteins, it represents a good model for studying the sequence properties and mechanisms underlying CAHS protein function. Furthermore, since CAHS D is protective during desiccation and is known to adopt transient helical structure, especially within its linker region, it is a good model for testing the general link between an IDP's helicity and protective capacity during drying, though of course the equilibrium between disorder and helicity will vary from IDP to IDP.

2.2 | The helical linker region of CAHS D promotes protection of LDH during drying

To probe what sequence features and secondary structures promote CAHS D-mediated protection, we began by assessing which domain(s) (Files S1 and S2) of CAHS D are important in mediating protection during drying. To this end, we tested the ability of the wild-type protein as well as each of its three individual domains (the N-terminus, the helical linker region, and the C-terminus) to stabilize a labile enzyme, LDH during drying (Figure 2a). We observed that the wild-type protein as well as each of its isolated domains displayed concentration-dependent protection of LDH (Figure 2b) (Files S4 and S6). We next calculated a protective dose 50% (PD50, mM) for the wild-type protein and each of its isolated domains. The PD50 is the concentration at which a protectant preserves 50% of LDH's enzymatic activity, meaning a lower PD50 indicates higher protective capacity. We observed that the PD50 of these four protectants varied dramatically (Figure 2d). Relative to CAHS D, the N- and C-termini show significant decreases in protection (increases in PD50), while the linker region protects LDH functionality in a statistically similar fashion as wild-type CAHS D, although having a slightly higher PD50 (Figure 2d). Thus, from a statistical stand-point the linker region fully recapitulates the protective capacity of wild-type CAHS D for protecting LDH.

To further assess the contribution of the helical linker in the context of the full-length protein (e.g., with an N- and C-termini), we utilized two variants, 2X LR and Ash1 LR (Figure 2A). 2X LR, is a variant of CAHS D generated by the tandem duplication of the helical linker region (Packebush et al., 2023). Ash1 LR is a variant generated by replacing the endogenous linker of CAHS D with a duplicated portion of the Ash1 domain of ASH1 (UniProt P34233), a protein involved in transcriptional regulation in *S. cerevisiae* with no connection to desiccation tolerance (Chandarlapaty & Errede, 1998). This insertion of Ash1 sequence results in a variant of 227 amino acids, the same length as wild-type CAHS D (Files S1 and S2). In both the 2X LR and Ash1 LR variants, the altered linker regions are flanked by the endogenous N- and C-termini of CAHS D. Consistent with the endogenous helical linker region promoting protection during drying, the 2X LR variant's PD50 is lower, but statistically similar to that of CAHS D, reinforcing the idea that linker constitutes the protective portion of CAHS D (Figure 2c,d). This is in contrast to the Ash1 LR, which provided significantly worse protection compared to wild-type CAHS D (Figure 2c,d).

Combined, these experiments identify the helical linker region of CAHS D as the major driver of LDH protection during drying.

2.3 | Helicity of CAHS D and its variants correlates with their protective capacity

We wondered what properties of our variants described in Figure 2 correlate with protective capacity during desiccation. To begin to assess this, we asked whether the

TABLE 1 Physical and structural parameters of full-length CAHS proteins.

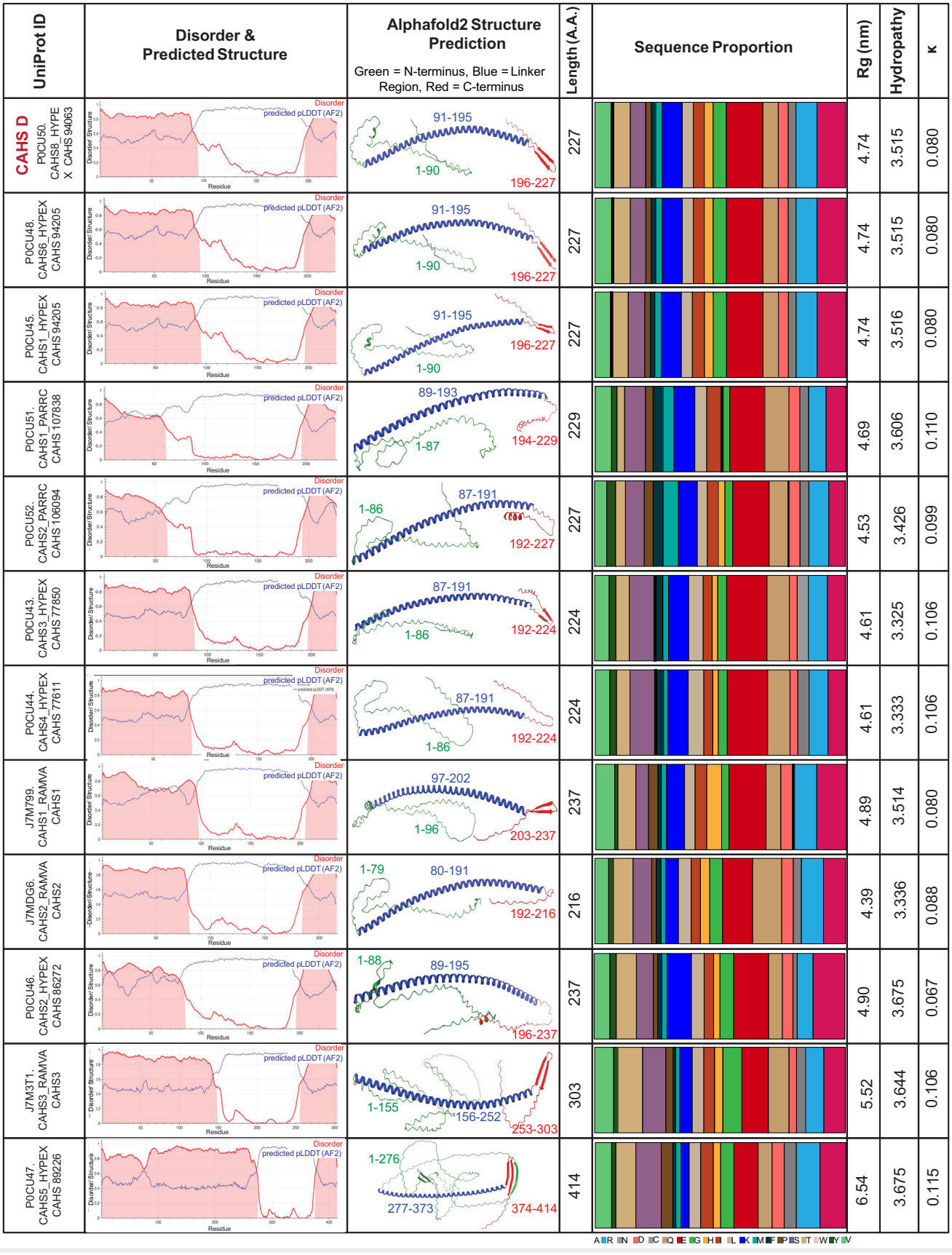

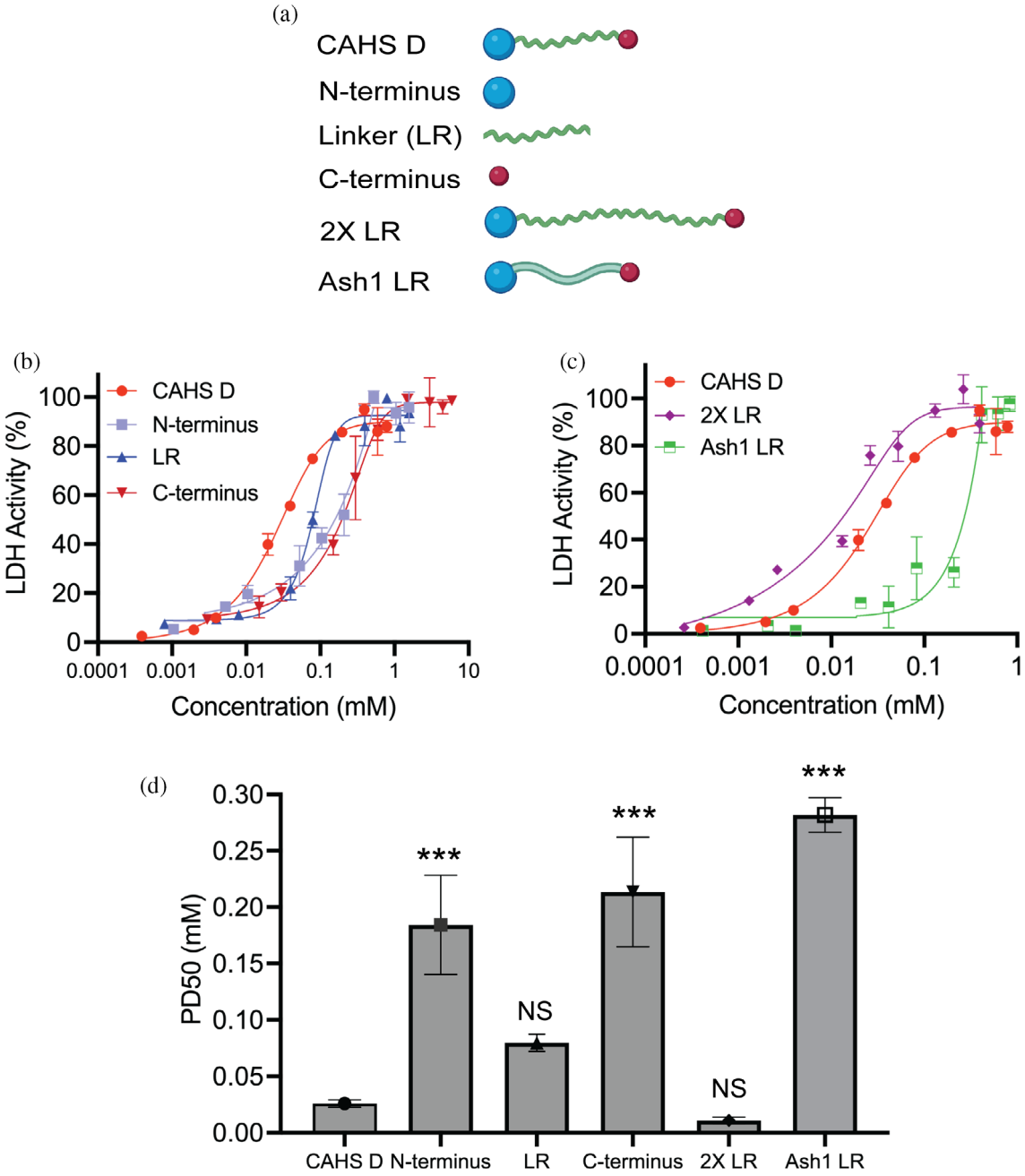

FIGURE 2 CAHS D Linker Region outperforms other domains in LDH protection assay. (a) Graphical representation of CAHS D domain evaluation variants. (b) Concentration dependence of LDH protection by CAHS D domains. (c) 50% protective dose (PD50, mM) for CAHS D variants. (d and e) Concentration dependence of LDH protection by CAHS D variants. $n = 3$, error bars represent standard deviation (SD). One-way ANOVA with Tukey's post hoc test, ns = not significant, ≥0.05 = not significant (ns), (0.01–0.05) = *, (0.001–0.01) = **, <0.001 = ***. CD, circular dichroism; LDH, lactate dehydrogenase; LR, linker region.

length of a variant correlates with its protection (Figure 3a). While there is a strong correlation between the length of variants containing endogenous CAHS D sequence and protective capacity ($R^2 = 0.8$, p value = 0.04; Figure 3a, blue), we observed that the Ash1 LR variant, which contains exogenous sequence, weakened this correlation ($R^2 = 0.23$, p value = 0.34; Figure 3a, red). This observation implies that beyond length, there is some property(s) that promote CAHS D-mediated protection.

Since CAHS D (as well as other CAHS proteins) is known to be partially helical (Eicher et al., 2022; Malki et al., 2022; Sanchez-Martinez, Nguyen, et al., 2023; Tanaka et al., 2022; Yamaguchi et al., 2012) and helicity has been proposed to be linked to the protective capacity of IDPs during drying (LeBlanc & Hand, 2021), we asked

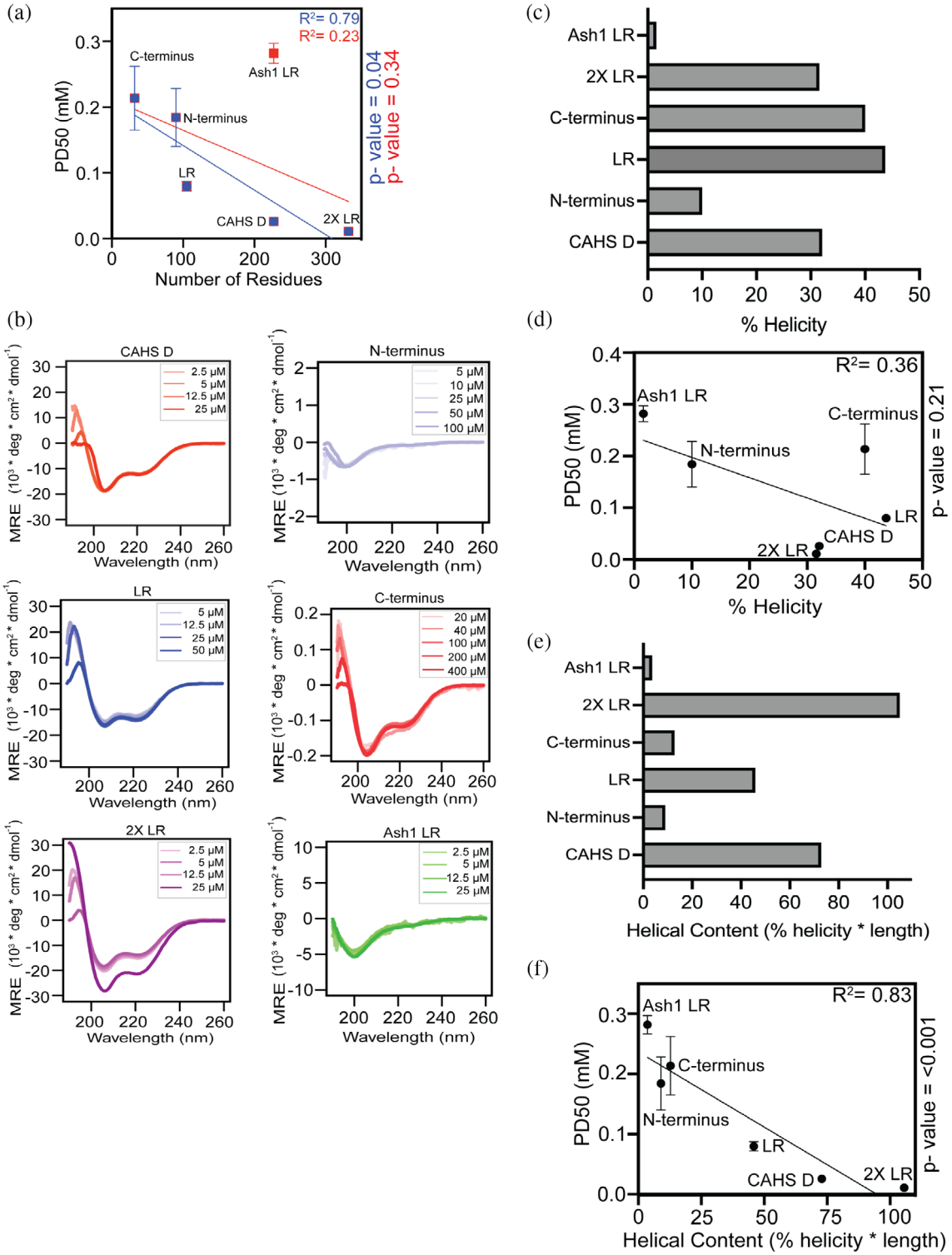

FIGURE 3 Helicity in the linker region is a potential property for protection. (a) Number of amino acid residues versus PD50 (mM) correlation plot. (b) CD spectra for CAHS D domain evaluation variants over a range of concentrations. (c) Percent helicity deconvoluted from CD spectra from (b). (d) Correlation between percent helicity and PD 50 (mM). (e) Helical content (% helicity * length) of different CAHS D variants. (f) Correlation between PD50 (mM) and helical content. All error bars represent mean ± SD. CD, circular dichroism.

if the helicity of our variants correlates with protection. To test this, we first performed circular dichroism (CD) spectroscopy on each of our variants (Figure 3b) (File S5). Spectra were obtained over a 10-fold concentration range to test for structural change that may occur due to self-association. No significant structural change is

seen for any of the variants in the concentration range tested (Figure 3b). Raw CD spectra were deconvolved allowing us to derive an estimate of the percent helicity of each variant (3C). Correlating percent helicity to protection did not result in a compelling trend ($R^2 = 0.36$, p value = 0.21; Figure 3d).

Seeing that percent helicity and protection do not correlate might well imply that helicity is unimportant for protection. However, we reasoned that protection is likely a function of both a protein's length and its percent helicity. For example, if two proteins are both 10% helical but one is 10 amino acids and the other 1000, the 1000 amino acid protein will on average have much more helical content. If helicity is important for protection during drying then both percent helicity and the length of a protein likely need to be taken into account.

To this end, we calculated the helical content (percent helicity × length) for each variant (File S4). These calculations revealed a decrease in the helical content in Ash1 LR as compared to CAHS D and linker region (Figure 3e). Consistent with the linker region containing a significant degree of helicity, our 2X LR variant contained two times the amount of helical content as the linker region alone (Figure 3e). Furthermore, terminal regions of CAHS D in isolation display lower levels of helical content as compared to the wild-type protein or the linker region (Figure 3e). Relating the protective capacity (PD50) of each of these CAHS D variants with their helical content resulted in a robust correlation ($R^2 = 0.83$; p value <0.001; Figure 3f).

Taken together, these results suggest that the helicity of CAHS D may contribute to its protective capacity during drying.

2.4 | Helicity of the CAHS D linker is necessary for robustly protecting LDH during desiccation

We sought to further probe the link between helicity of the linker region of CAHS D and its protective capacity during drying by generating mutants specifically designed to reduce helical content while maintaining as much endogenous sequence composition and grammar as possible. These mutants consist of either the full-length CAHS protein or linker region in isolation with helix-breaking proline residues replacing endogenous residues at every five to eight residues within the linker region (Files S1 and S2). These variants we term full-length linker region proline (FL_LR_P) and linker region proline (LR_P), respectively. In these variants, the replacement of endogenous residues with proline maintains the total amino acid number, but modestly increases the isoelectric point and molecular weight of the resulting protein (Table 2).

We began characterizing FL_LR_P and LR_P variants by assessing their helical content using CD spectroscopy (Figure 4a,b) (File S5). Consistent with previous reports that prolines are potent disruptors of secondary structure (Deber et al., 2010; Woolfson & Williams, 1990), we observed a decrease in helical content to negligible levels

TABLE 2 Physicochemical features of CAHS D variants used in the study.

Variants	AA residue number	Isoelectric point (p^I)	MW (Da)	Helical content (% helicity * length)
CAHS D	227	5.98	25,485.32	72.9
N-terminus	90	6.02	9547.62	9
LR	105	6.07	12,620.11	45.9
C-terminus	32	5.45	3353.62	12.8
2X LR	332	6	38,160.47	105
Ash1 LR	227	10.84	24,119.87	3.6
FL_LR_P	227	6.12	25,652.75	6.3
LR_P	105	6.91	12,787.54	2.7
FL_LR_NH	227	5.98	24,845.60	2.7
LR_NH	105	6.06	11,980.39	1.1
LR_KtoR	105	6.07	12,956.27	41.5
LR_RtoK	105	6.07	12,199.91	19.1
LR_DtoE	105	6.10	12,690.25	31.7
LR_EtoD	105	5.85	12,311.52	8

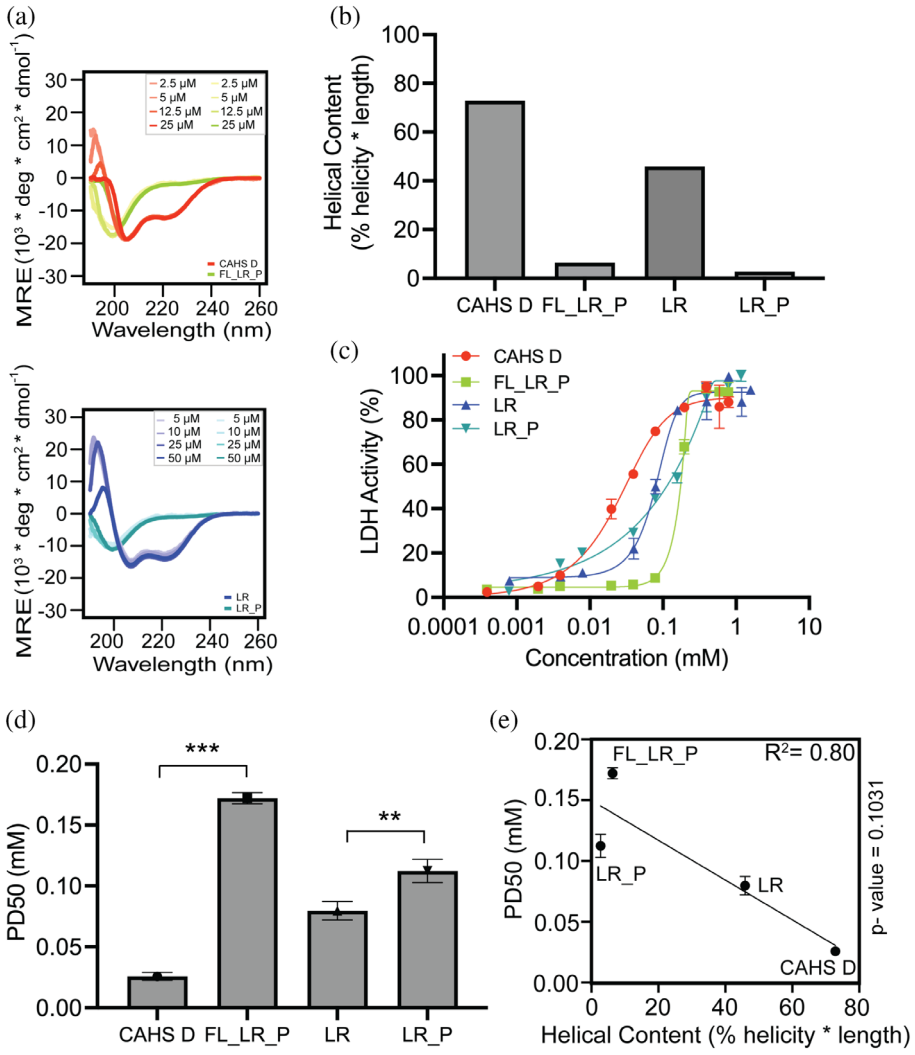

FIGURE 4 Helix disrupting sequence variations disrupt protection. (a) CD spectra of full-length (top) and linker (bottom) proline insertion variants, as well as wild-type proteins. (b) Helical content deconvoluted and normalized from CD spectroscopy data. (c) Concentration dependence of proline insertion variants in protecting LDH during drying. (d) PD50 value calculated from fitted sigmoidal curve from (c). One-way ANOVA with Tukey's post hoc test, $n = 3$; ns = not significant, ≥0.05 = not significant (ns), (0.01–0.05) = *, (0.001–0.01) = **, <0.001 = ***. (e) Correlation between PD50 (mM) and helical content (% helicity * length). $n = 3$, All error bars represent mean ± SD. p Value: ≥0.05 = not significant, (0.01–0.05) = *, (0.001–0.01) = **, <0.001 = ***. $N = 3$, All error bars represent mean ± SD. CD, circular dichroism; LDH, lactate dehydrogenase.

in both our FL_LR_P and LR_P variants (Figure 4b). Here, as before, no change in CD spectra was observed over the range of concentrations tested (Figure 4b).

Next, we performed LDH desiccation assays to assess how direct disruption of helicity within the context of wild-type CAHS D, or the linker region in isolation, affects the protective capacity of these IDPs. In both cases, we observed significant decreases in the protective capacity of FL_LR_P and LR_P relative to both wild-type CAHS D and the linker region in isolation, represented by a significant increase in the PD50 value for each variant (Figure 4c,d) (Files S4 and S6). Furthermore, the correlation of the helical content of wild-type CAHS D, its linker region, and the proline variants with protective capacity shows a trend with an R^2 value of 0.80, but with a p value of >0.05 (Figure 4e).

Taken together, these results suggest that the helicity of CAHS D, and in particular the linker region of CAHS D, promotes protection of LDH during drying, but is not the only feature governing protective capacity.

2.5 | Sequence identity of charged residues in the CAHS D linker promotes helical structure and protection during drying

After observing that direct disruption of helicity within the linker region of CAHS D results in a loss of protective capacity during drying, we were curious about what sequence features within the linker promote helicity. To this end, we examined the primary sequence of CAHS D and its linker more closely.

Analysis of the linker region sequence using CIDER (Holehouse et al., 2017) reveals a high fraction of charged residues (FCR = 0.524) and characterizes this domain as a strong polyampholyte (sequence containing positively and negatively charged amino acids) (Das & Pappu, 2013). The amino acid sequences of polyampholyte helices have been found to have a high amount of glutamate (E) and both positively charged lysine (K) and arginine (R) residues in a regular, repeating pattern of

oppositely charged residues (Batchelor & Paci, 2018). Consistent with this, out of the high fraction of charged residues in the linker region of CAHS D, there is an approximately equal amount of positively charged K and R (12:15) residues, whereas for negatively charged amino acids, there is a bias for E relative to D (22:6) residues (Figure 1b,c). Thus, the ratio and identities of charged residues within the linker region of CAHS D mirrors that of traditional polyampholyte helices.

To test the contribution of charge identity to the helical nature of CAHS D's linker region as well as to desiccation protection, we generated four charge identity variants. These variants, called LR_KtoR, LR_RtoK, LR_EtoD, and LR_DtoE, were generated by replacing all the Ks for Rs (and vice versa) or all the Es for Ds (and vice versa) within the isolated linker region (Files S1 and S2). These mutants maintain the length and charge of the linker region and allow us to further test the relationship between sequence features, helicity, and protective capacity of the CAHS D linker region during drying.

To begin, we tested the effect of these charge identity variants on helicity using CD spectroscopy. CD spectroscopy revealed that changing the identity of charged residues, while still maintaining overall charge influences the helicity of the linker region (Figure 5a,b) (Files S4 and S5). Specifically, disruption of the highly biased presence of E, by replacement with D, showed a decrease in helical content in LR_EtoD as compared to the wild-type linker region. The converse was also true, as replacing the relatively few D residues in the linker region with E residues (LR_DtoE) also reduced the helical content. However, LR_DtoE maintained more helicity than LR_EtoD, which is consistent with a recent study suggesting that glutamate helps maintain helicity, while aspartate helps maintain extended structures in IDPs (Roesgaard et al., 2022). This trend partially carried over to positively charged residues as well, with our LR_RtoK variant showing reduced helical content, while the helical content of the LR_KtoR variant remained more or less consistent with that of the wild-type linker region.

Next, we tested the protective capacity of these four charge identity variants using the LDH assay. We observed significant decreases in protective capacity for all charge identity variants except LR_KtoR (Figure 5c,d). Correlative analysis comparing the helical content and PD50 of these variants revealed a strong correlation ($R^2 = 0.9$; p value <0.02) between these properties (Figure 5e).

These results demonstrate that charge identity contributes to helicity of the CAHS D linker region. Furthermore, these results provide further evidence that helicity is linked to the protective capacity of the CAHS D linker during drying.

2.6 | Removal of hydrophobic residues does not rescue loss-of-helicity variants

Our results thus far implicate helicity as an important feature in determining the protective capabilities of CAHS D. One possible interpretation is that transient helicity ensures CAHS linker residues are exposed along helical faces and therefore primed for inter-molecular interactions with clients such as LDH. Transient intra-molecular interactions driven by hydrophobic residues can lead to IDR compaction, which minimizes the potential for intermolecular interactions (Martin et al., 2020; Mok et al., 1999). If this is the case, loss of helicity may lead to aberrant intramolecular interactions driven by hydrophobic residues, which in turn could impede inter-molecular interactions and the protective capabilities of the linker region.

To test this hypothesis, we designed variants to simultaneously disrupt helicity and remove hydrophobic residues by replacing hydrophobic residues with either serine or the helix-breaking residue glycine. Variants of both the linker in isolation (LR_NH) and the linker in its endogenous context (FL_LR_NH) were designed. As predicted, these designs led to a dramatic decrease in helical content (Figure 6a,b; Files S1 and S2). Importantly, similar to our previous observations, we also measured a significant decrease in the protective capacity of FL_LR_NH compared to wild-type CAHS D as well as LR_NH compared to the linker region in isolation (Figure 6c–e) (Files S4, S5, and S6). These results further support a model in which helicity is critical for CAHS protective capabilities and suggest that aberrant intra-molecular interactions driven by hydrophobic residues do not underlie the reduced protection observed in low-helicity sequences.

3 | DISCUSSION

An emerging paradigm in the anhydrobiosis field is the prevalent enrichment of IDPs that help to mediate protection during drying (Hand et al., 2011; Hesgrove & Boothby, 2020; Romero-Perez et al., 2023). Transient helicity, and the acquisition of increased helical content during desolvation, has been reported in many desiccation-related IDPs spanning diverse families (Bremer et al., 2017; Shimizu et al., 2010; Tunnacliffe et al., 2010; Yamaguchi et al., 2012). Helical structure has often been speculated to be essential for desiccation-related IDP function during drying, but direct, empirical evidence demonstrating this linkage is lacking. Here we show that helical structure found in the linker regions of CAHS D, a desiccation-related IDP required for tardigrades to survive drying, is necessary to robustly protect the labile enzyme LDH during drying.

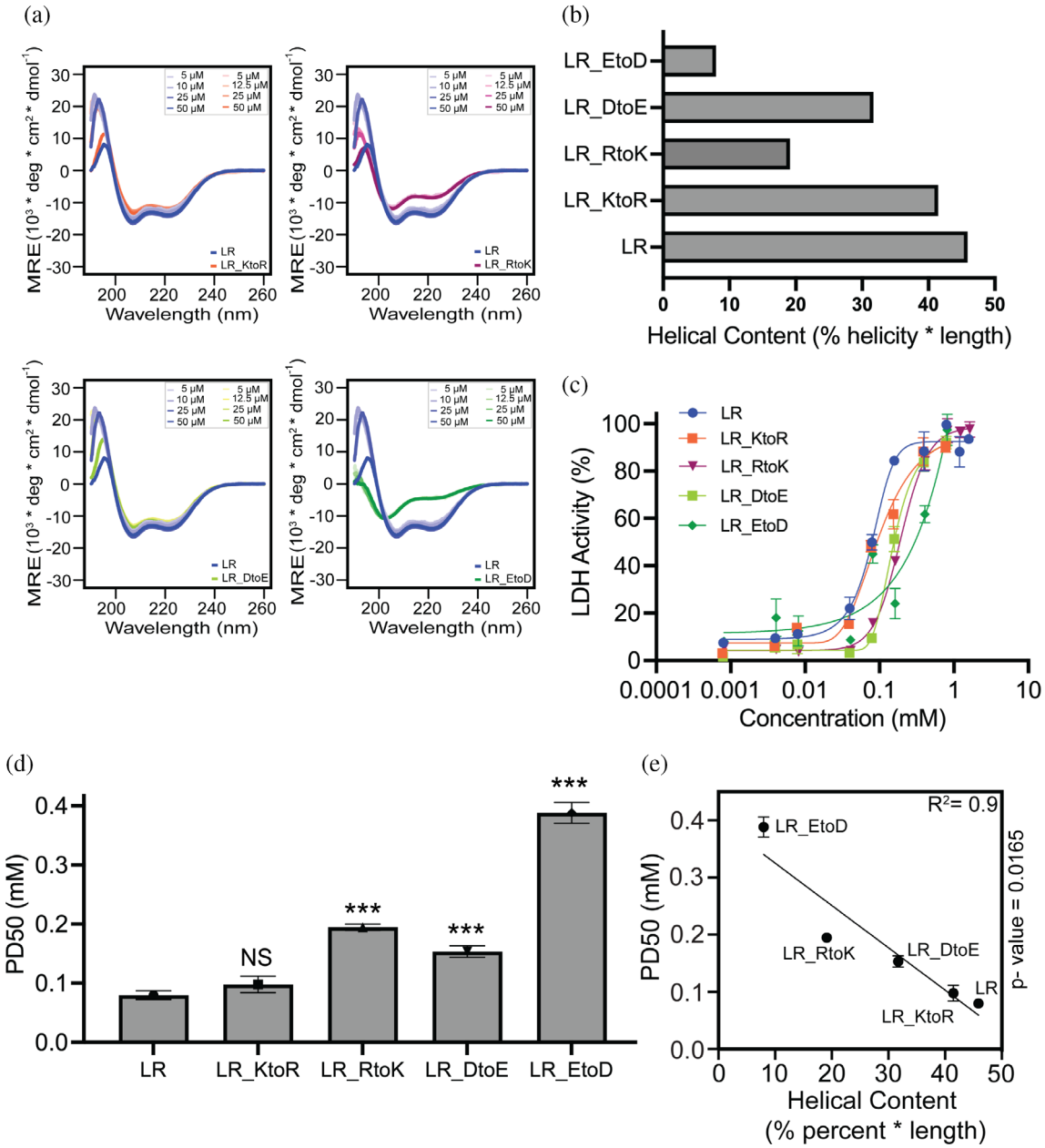

FIGURE 5 Charge identity defines fine-tuning of helix formation in CAHS D linker region. (a) CD spectra of CAHS D linker region charge identity variants. (b) Helical content deconvoluted and normalized from CD spectroscopy data. (c) Sigmoidal curve representing LDH unfolding protection. Protection is plotted as the mean percentage of LDH enzyme activity against a range of concentrations in mM. (d) PD50 (mM) calculated from the fitted sigmoidal curve from (c). One-way ANOVA with Tukey's post hoc test, ns = not significant, ≥0.05 = not significant (ns), (0.01–0.05) = *, (0.001–0.01) = **, <0.001 = ***. (e) Correlation between PD50 and helical content. *p* Value: ≥0.05 = not significant, (0.01–0.05) = *, (0.001–0.01) = **, <0.001 = ***. $N = 3$, All error bars represent mean ± SD. CD, circular dichroism; LDH, lactate dehydrogenase.

3.1 | The linker region is the protective domain of CAHS D

CAHS D has previously been shown to be essential for robust anhydrobiosis in the tardigrade *H. exemplaris*, to increase desiccation tolerance in heterologous systems, and to be sufficient to protect labile enzymes in vitro (Boothby et al., 2017). Furthermore, CAHS D occupies a dumbbell-like ensemble of interconverting conformations, composed of two collapsed termini held apart by an extended linker region (Sanchez-Martinez, Nguyen, et al., 2023). However, previous studies have not examined which of these three domains contribute to the protective capacity of CAHS D. Nor have they examined

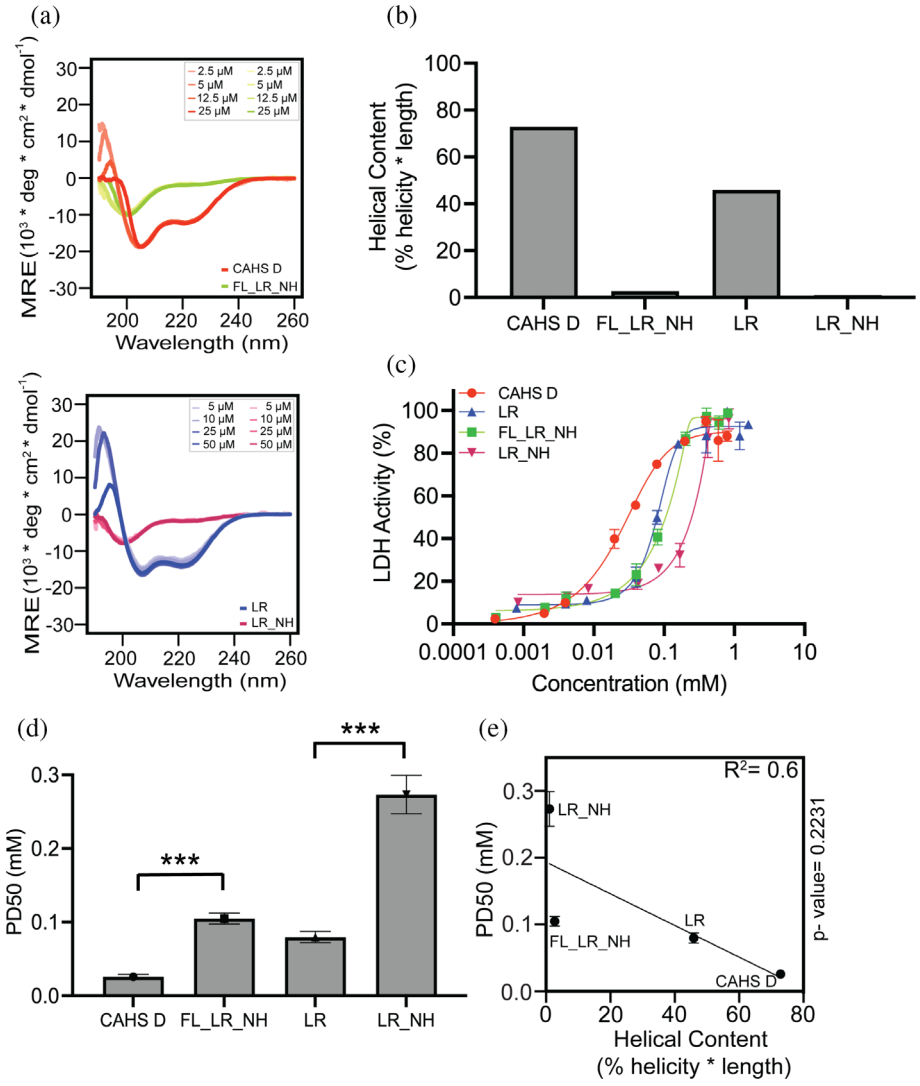

FIGURE 6 Removal of hydrophobic residues does not rescue loss-of-helicity variants. (a) CD spectra for no hydrophobic variants, as well as wild-type proteins. (b) Helical content deconvoluted and normalized from CD spectroscopy data. (c) Sigmoidal curve representing LDH unfolding protection. Protection is plotted as the mean percentage of LDH enzyme activity against a range of concentrations in mM. (d) PD50 value calculated from the fitted sigmoidal curve. One-way ANOVA with Tukey's post hoc test, ns = not significant, ≥0.05 = not significant (ns), (0.01–0.05) = *, (0.001–0.01) = **, <0.001 = *** (e). Correlation between PD50 and helical content. *p* Value: ≥0.05 = not significant, (0.01–0.05) = *, (0.001–0.01) = **, <0.001 = ***. $N = 3$, All error bars represent mean ± SD. CD, circular dichroism; LDH, lactate dehydrogenase.

what sequence features, including helicity, are important for CAHS D-mediated desiccation tolerance.

In our current study, we show that statistically the linker region of CAHS D preserved LDH function to a similar degree as wild-type CAHS D. Furthermore, either of the terminal regions of CAHS D in isolation protects LDH far worse than the wild-type protein. Furthermore, replacement of the linker region with an exogenous sequence results in large decreases in protection. From this, we infer that the domain which most prominently drives CAHS D-mediated protection is the internal linker region.

3.2 | Reducing helicity of the CAHS D linker results in a loss of protective capacity

Replacing the endogenous linker of CAHS D with a novel sequence or altering the sequence of the linker either by insertion of helix-breaking prolines, swapping charged amino acid identities, or by replacement of hydrophobic residues with helix-breaking glycines or serines results in significant decreases in helicity and in protective capacity. These experiments imply that the composition of the linker is important for protection. Coupled with biophysical assessment of secondary structure, an overarching conclusion from these sequence variants and functional studies is that sequence features promoting helicity also promote protection.

Here, the observed sequence features and composition underlying CAHS D linker helicity is in line with previous reports. For example, in silico analysis of sequences containing glutamate (E) are predicted to have greater helicity than those containing aspartate (D) (e.g., $(E_4K_4)_2$ vs $(D_4K_4)_2$), while sequences containing arginine have a higher predicted helicity than those containing lysine (e.g., $(D_4R_4)_2$ vs $(D_4K_4)_2$) (Batchelor & Paci, 2018). Within the linker of CAHS D, there is a clear bias for negatively charged E relative to D (22:6), which

should promote helicity. Consistent with this, converting all E residues to Ds within the linker (LR_EtoD) results in a dramatic loss of helicity (and protection) relative to converting D to E (LR_DtoE). Whereas, converting all K residues to R (LR_KtoR) has little effect on helical content, while the converse (LR_RtoK) dramatically decreases linker helicity.

3.3 | Helicity drives, but is not the only property contributing to, desiccation tolerance

In this study, each perturbation to the wild-type CAHS D sequence which decreased helical content resulted in a decrease in protection, while increasing helicity resulted in an increase in protection, albeit with varying degrees of significance. Comparison of the protective capacity (PD50) and helical content of each variant used in this study shows a significant correlation (p value = 0.02), indicating that helicity is linked to the protective capacity of CAHS D and its variants (Figure 7). However, the R^2 value for this correlation is only 0.46, indicating that while helicity significantly correlates with protection, it is likely not the only sequence feature or property of CAHS D responsible for promoting protection. This conclusion provides insights into the necessity of these structural and biophysical properties not only for CAHS proteins, but also potentially for other stress-related IDPs, such as LEA proteins.

With this in mind, it is important to consider how the helicity of CAHS D, and particularly the linker region, compares to the helicity of other desiccation-related IDPs (e.g., LEA proteins). Helicity in LEA proteins has historically been viewed as transient and/or induced by desiccation. These insights are largely based on structural studies performed in the desolvating agent trifluoroethanol (TFE), which is used by some to simulate desiccation, but in reality simply induces a hydrophobic environment (Bremer et al., 2017; Koubaa et al., 2019; Tanaka et al., 2022). Many LEA proteins adopt helical conformations with increasing levels of TFE, which is also seen in CAHS proteins (Wang et al., 2023; Yamaguchi et al., 2012). Structural predictions as well as residue level NMR suggest a high level of helicity within the linker of CAHS D (Malki et al., 2022), which may, contrary to TFE results, suggest that the helicity of the CAHS D linker is more stable than some LEA proteins. Even within LEA protein families, there is variation in the degree of disorder and helicity observed for these proteins. Thus, while CAHS D is a desiccation-related IDP with helical content, it remains to be determined how much these properties make it (or any IDP for that matter) an ideal model for all other desiccation-related IDPs.

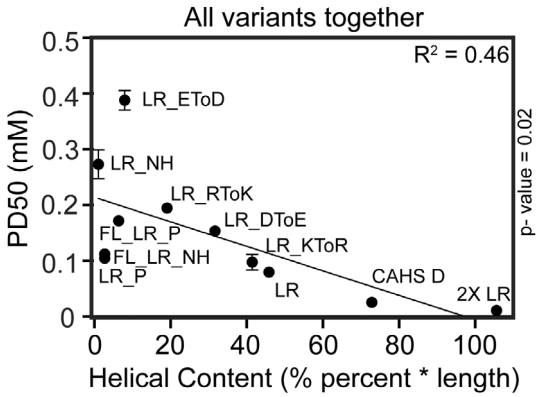

FIGURE 7 Correlation of protective dose 50 and helical content for all variants used in this study. Correlation of PD50 and helical content for all variants. p Value: ≥0.05 = not significant, (0.01–0.05) = *, (0.001–0.01) = **, <0.001 = ***. All error bars represent mean ± SD.

One commonality shared between the helices formed by the CAHS D linker and other desiccation-related IDPs, such as LEA proteins, is their amphipathic nature. Amphipathicity of LEA proteins has previously been proposed to allow for hydrophobic interactions between LEA proteins and client molecules (e.g., membrane headgroups) and could play a role in self-assembly of proteins into oligomers (Shou et al., 2019; Tunnacliffe & Wise, 2007). While no evidence to date exists that CAHS D, or its linker region, interacts with membranes, several studies have demonstrated that CAHS D, as well as other CAHS proteins, oligomerize (Eicher et al., 2022; Malki et al., 2022; Sanchez-Martinez, Nguyen, et al., 2023; Tanaka et al., 2022; Yagi-Utsumi et al., 2021). Furthermore, the helicity and amphipathic nature of the linker region of CAHS D and other CAHS proteins has been shown to be essential for oligomerization into higher-order structures (Sanchez-Martinez, Nguyen, et al., 2023; Tanaka et al., 2022). Thus, one might speculate that the reason behind a decrease in protection upon helix-disruption is due to a loss in the ability to oligomerize. However, we found this not to be the case (Figure S1–S4). This is consistent with previous observations that while oligomerization can promote some forms of CAHS-mediated stress tolerance, oligomerization is not essential for protection (Hesgrove et al., 2021; Sanchez-Martinez, Nguyen, et al., 2023).

3.4 | Beyond helicity and secondary structure

While many desiccation-related IDPs have been shown to possess transient helicity, which increases upon drying,

this is by no means an absolute rule. For example, SAHS proteins from tardigrades contain more stable beta-structure (Fukuda et al., 2017; Fukuda & Inoue, 2018; Miyazawa et al., 2021; Miyazawa et al., 2022), as do some LEA proteins (Furuki & Sakurai, 2014). Even CAHS proteins are known to contain transient beta-structure, albeit localized to their terminal regions (Eicher et al., 2022; Sanchez-Martinez, Nguyen, et al., 2023). How transient secondary structure beyond helices influences or promotes the protective capacity of IDPs during drying is unknown.

As touched upon above, many desiccation-related IDPs are known oligomerize. So these IDPs go beyond forming simple dimers or trimers and form higher-order oligomers (Belott et al., 2020; Eicher et al., 2022; Malki et al., 2022; Sanchez-Martinez, Nguyen, et al., 2023; Tanaka et al., 2022; Yagi-Utsumi et al., 2021). In the case of CAHS D and some LEA proteins, this results in the formation of a gel-like network (Belott et al., 2020; Eicher et al., 2022; Malki et al., 2022; Sanchez-Martinez, Nguyen, et al., 2023; Tanaka et al., 2022; Yagi-Utsumi et al., 2021). The adoption of such higher-order quaternary structure, either through helical interactions or other means, is likely to also play a role in promoting protection during drying (Belott et al., 2020; Eicher et al., 2022; Malki et al., 2022; Sanchez-Martinez, Nguyen, et al., 2023; Tanaka et al., 2022; Yagi-Utsumi et al., 2021). The formation of these higher-order structures, at least for CAHS proteins, has been proposed to mediate desiccation tolerance at the protein level through several potential mechanisms including: coordination of water, providing a matrix for entrapment, or induction of a viscous state that slows unfolding/aggregation (Boothby, 2021; Boothby et al., 2017; Packebush et al., 2023; Piszkiewicz et al., 2019; Sanchez-Martinez, Ramirez, et al., 2023). It should be noted that these mechanisms of protein protection are not mutually exclusive, and CAHS oligomerization may confer protection at additional scales, for example, at the cellular level via the formation of a cytoskeletal-like network and/or induction of biostasis (Eicher et al., 2022; Sanchez-Martinez, Nguyen, et al., 2023; Tanaka et al., 2022; Yagi-Utsumi et al., 2021).

Thus, while our study shows empirically that helicity of CAHS D, a desiccation-related IDP, is linked to its protective capacity, it also demonstrates that other properties likely play a role in CAHS D-mediated desiccation tolerance. Future work identifying what these additional properties are will be of great interest to the anhydrobiosis field, and will likely need to take into account the role of helices in mediating survival and protection during extreme drying.

4 | MATERIALS AND METHODS

4.1 | Sequence analysis

CAHS proteins' sequences were obtained from the UniProt database (https://www.uniprot.org/). Protein parameters were computed using Expasy ProtParam tool (Walker, 2007). Intrinsic disorder and predicted structure were predicted using metapredict online (v2.3) (Emenecker et al., 2021). Parameters related to disordered protein sequence such as kappa (κ) value, hydropathy, and diagram of states were calculated using CIDER (Holehouse et al., 2017). Protein structure was predicted by Alphafold2 (Mirdita et al., 2022) and visualized using ChimeraX (Pettersen et al., 2021). Hydrophobic moment of the CAHS D sequence was calculated and plotted using the EMBOSS hmoment calculator (Eisenberg et al., 1982). (https://www.bioinformatics.nl/cgi-bin/emboss/hmoment)

4.1.1 | Multiple sequence alignment

Multiple sequence alignment of the CAHS D and its variants used in the study was run using UniProt ClustalO Multiple Sequences Alignment tool. https://www.expasy.org/resources/uniprot-clustalo

4.2 | Sequence design tool: Charge identity mutants, hydrophobic residue mutants

Synthetic disordered proteins were designed using GOOSE, a tool for the rational design of synthetic disordered proteins (https://github.com/idptools/goose). In all cases, disorder was revaluated using metapredict (Emenecker et al., 2021), and designs were generated using GOOSE' variant design feature.

4.3 | CAHS D variants' construct design, cloning, and −80°C freezer stock preparation

Escherichia coli codon-optimized gBlocks encoding CAHS D and its mutant proteins used in this study were synthesized by (Integrated DNA Technologies) and cloned into pET-28 b (+) vector (Addgene) for bacterial expression. Plasmids containing CAHS D or its variants were transformed initially into DH5α *E. coli*, plated onto Kanamycin (Kan) containing LB agar plates. Selected colonies were grown overnight in the LB broth followed by plasmid extraction for the sequence confirmation (Eton

Bioscience). Sequence verified plasmids were then transformed into BL21 (DE3) *E. coli* expression strains. BL21 (DE3) transformed colonies from LB+ Kan plates were verified by a small scale protein expression test, and successful colonies were used to make −80°C freezer stocks.

4.4 | Expression

About 10 mL of saturated overnight (16 h) culture of the respective CAHS D variant was used to inoculate 1 L of LB broth (10 g/L peptone, 5 g/L yeast, and 5 g/L NaCl) supplemented with Kanamycin to a final concentration of 50 μg/mL. The cultures were shaken (180 rpm) at 37°C until the optical density at 600 nm was 0.6 (not higher than 0.8). Once the cultures reached the expected OD, a final concentration of 1 mM IPTG was used to induce the target protein expression. After 4 h, the cells were collected as pellets by centrifuging at 4000 rpm for 30 min at 4°C. The cell pellets from 1 L culture were resuspended into 5 mL of 20 mM Tris (pH 7.5) and mixed with 30 μL of 1× protease inhibitor (Sigma-Aldrich).

4.5 | Protein purification

Resuspended cell pellets were heat shocked at 95°C for 15 min and spun down at 10,500 rpm for 30 min at 10°C followed by a 0.22-μM syringe filtration (EZFlow Syringe Filter, Cat. 388-3416-OEM). The heat-soluble supernatant was mixed with 2× volume of 8 M urea (Acros Organics, CAS no. 57-13-6), 50 mM sodium acetate (Sigma-Aldrich, Lot #SLCF 1907, Japan) buffer (pH 4.0). For Ash1 LR, the heat soluble supernatant was mixed with 2× volume of 8 M Urea, 20 mM Tris-base buffer with a pH of 7.5. The protein sample in urea was further purified on Cytiva AKTA Pure chromatography system (UNICORN 7 Workstation pure-BP-exp (Cytiva, Cat. #29128116, USA) using a cation exchange column (Cytiva HiPrep™, SP HP 16/10, Cat. #29018183). The proteins were eluted using gradients of 1 M NaCl. Different CAHS D variants will elute at different salt concentrations using a gradient of 0%–50% of respective buffers with 1 M NaCl. SDS-PAGE was used to identify fractions containing pure CAHS D or its mutant variants. Confirmed fractions were pooled, transferred to a dialysis tubing of 3.5 kDa membrane pore size (SpectraPor 3 Dialysis Membrane, Part No. 132724; FL, USA) and dialyzed against 20 mM Phosphate buffer (pH 7) for at least 4 h, followed by 6 rounds of 4 h dialysis against Milli Q H_2O (18.2 MΩ cm). Dialysate containing purified CAHS D variant concentration was then quantified fluorometrically using Qubit 4 fluorometer (Invitrogen, REF Q33226) utilizing Qubit™ Protein Assay Kit (Catalog number Q33211, Thermo Fisher Scientific, USA), flash-frozen and lyophilized (Labconco FreeZone 6, Cat. 7752021; USA) for 48 h before storage at −20°C.

4.6 | LDH assay

LDH activity assay was based on the procedure outlined by Goyal et al. (2005). Lyophilized CAHS D and its mutants' were resuspended into 25 mM Tris–HCl (pH 7) and concentrations were quantified using Qubit™ Protein Assay Kit (Catalog number Q33211, Thermo Fisher Scientific, USA) and measured fluorometrically by Qubit 4 fluorometer (Invitrogen, REF Q33226, Thermo Fisher Scientific; USA). Rabbit Muscle L-LDH (Sigma-Aldrich, REF 10127230001, Millipore Sigma, USA) was mixed to a range of sample protein concentrations having a final concentration of 0.1 g/L. The range of sample concentration for CAHS D, FL_LR_P, and FL_LR_NH used in this assay is (0.01–20) g/L, whereas for CAHS D w/Ash1, LR and all its variants it is (10–0.01) g/L. The final volume of 0.1 g/L LDH mixed with (20/10–0.01) g/L test variants is 100 μL. Half of the sample was stored at 4°C, and the other half was desiccated using speedvac for 16 h without heating (SAVANT Speed Vac Concentrator, Thomas Scientific, USA) with OFP400 vacuum pump (Thermo Fisher Scientific, USA). Desiccated samples were rehydrated with 250 μL molecular grade H_2O, whereas unstressed control samples stored at 4°C were diluted with 200 μL of molecular grade H_2O, and all samples were kept on ice until the enzymatic activity was measured. To check the LDH activity, 10 μL of the sample was added to a mixture containing 980 μL of pyruvate phosphate buffer (100 mM sodium phosphate, 2 mM sodium pyruvate; pH 6.0) and 100 μM NADH (Sigma-Aldrich NADH; disodium Salt, grade II) in a quartz cuvette and the enzyme kinetics was measured. LDH enzyme activity in the conversion of pyruvate to lactate is calculated by measuring the loss of NADH at UV absorbance of 340 nm using nanodrop (Thermo Scientific NanoDrop One, USA) at every 2 s for a kinetic loop of 1 min. The activity was determined as a ratio of NADH loss in stressed samples compared to the controls. LDH activity was measured in triplicates for each sample concentration for all different CAHS D variants.

4.7 | Circular dichroism spectroscopy

Lyophilized CAHS D and its variants were resuspended in tris buffer pH 7 to a concentration of 25 μM. Protein concentrations were quantified using Qubit™ Protein Assay

(Catalog number Q33211, Thermo Fisher Scientific, USA). The suspension was then diluted with a 25 mM Tris buffer, pH 7 to concentrations ranging from (2.5–25) μM for measurement. Aliquots of each concentration were measured in 1 and 0.05 mm quartz cuvettes in a circular dichroism spectrometer (Jasco, J-1500 model, Japan). Each measurement was performed in three replicates.

4.8 | Deconvolution of circular dichroism spectra and normalization of helical content

Beta Structure Selection method (BeStSel) was used to calculate the detailed structure information from the CD spectra (Micsonai et al., 2018). The deconvoluted percent of α-helix was normalized to the amino acid residue number of different CAHS D variants to calculate the helical content (% helicity * length).

4.9 | Data visualization and statistical analysis

CD spectroscopy data were plotted using R-Studio v1.3.1073 (File S3). Sigmoidal curve plotting, analysis of 50% protective dose value followed by data visualization, and regression analysis were done using GraphPad Prism v9.5.1. Statistical difference of PD50 value between variants was analyzed using one-way ANOVA with Tukey's post hoc test.

4.10 | BS^3 crosslinking experiment

BS^3 (bis[sulfosuccinimidyl] suberate) (Catalog A39266, Thermo Fisher Scientific, USA) having an arm of 11.4 Å amine ester crosslinker was used according to the manufacturer's instructions. A concentration of 1 mg/mL of each protein was mixed with a range (0.5–4 mM) of BS3 crosslinker. The samples were incubated for 30 min at room temperature; the reaction was stopped by adding a protein gel loading buffer (Bio-Rad catalog #1610737), and 20 μL of each sample was loaded onto the gel.

AUTHOR CONTRIBUTIONS

Thomas Boothby: Conceptualization; supervision; project administration; writing – review and editing; writing – original draft; funding acquisition. **Sourav Biswas:** Conceptualization; data curation; formal analysis; visualization; writing – original draft; methodology; investigation; writing – review and editing. **Edith Gollub:** Investigation; writing – review and editing. **Feng Yu:** Investigation; writing – review and editing. **Garrett Ginell:** Investigation; writing – review and editing. **Alex Holehouse:** Supervision; writing – review and editing. **Shahar Sukenik:** Supervision; writing – review and editing.

ACKNOWLEDGMENTS

We thank members of the Water and Life Interface Institute (WALII), supported by National Science Foundation DBI Grant 2213983, for helpful discussions, as well as support from the NSF via the IntBio research program under awards 2128069 to TCB, 2128067 to SS, and 2128068 to ASH. Fellowship to SB funded by Wyoming NASA EPSCoR, NASA Grant #80NSSC19M0061 supported this work. This work was supported by the USDA National Institute of Food and Agriculture, Hatch Project #1012152. Anja Thalhammer is thanked for her helpful discussions and insights.

CONFLICT OF INTEREST STATEMENT

The authors declare no conflict of interest.

ORCID

Sourav Biswas https://orcid.org/0000-0002-5571-2334
Thomas C. Boothby https://orcid.org/0000-0002-8807-3268

REFERENCES

Armstrong LE, Johnson EC. Water intake, water balance, and the elusive daily water requirement. Nutrients. 2018;10: 1928. https://doi.org/10.3390/nu10121928

Batchelor M, Paci E. Helical polyampholyte sequences have unique thermodynamic properties. J Phys Chem B. 2018;122:11784–91.

Battaglia M, Olvera-Carrillo Y, Garciarrubio A, Campos F, Covarrubias AA. The enigmatic LEA proteins and other hydrophilins. Plant Physiol. 2008;148:6–24.

Battista JR, Park MJ, McLemore AE (2001) Inactivation of two homologues of proteins presumed to be involved in the desiccation tolerance of plants sensitizes *Deinococcus radiodurans* R1 to desiccation. Cryobiology 43:133–9. Available from: https://pubmed.ncbi.nlm.nih.gov/11846468/

Belott C, Janis B, Menze MA. Liquid-liquid phase separation promotes animal desiccation tolerance. Proc Natl Acad Sci U S A. 2020;117:27676–84.

Boothby TC. Water content influences the vitrified properties of CAHS proteins. Mol Cell. 2021;81:411–3.

Boothby TC, Pielak GJ. Intrinsically disordered proteins and desiccation tolerance: elucidating functional and mechanistic underpinnings of anhydrobiosis. BioEssays. 2017;39:1700119. https://doi.org/10.1002/bies.201700119

Boothby TC, Tapia H, Brozena AH, Piszkiewicz S, Smith AE, Giovannini I, et al. Tardigrades use intrinsically disordered proteins to survive desiccation. Mol Cell. 2017;65:975–984.e5.

Bremer A, Wolff M, Thalhammer A, Hincha DK (2017) Folding of intrinsically disordered plant LEA proteins is driven by glycerol-induced crowding and the presence of membranes.

FEBS J 284:919–36. Available from: https://pubmed.ncbi.nlm.nih.gov/28109185/

Browne J, Tunnacliffe A, Burnell A. Plant desiccation gene found in a nematode. Nature. 2002;416:38.

Caprioli M, Krabbe Katholm A, Melone G, Ramløv H, Ricci C, Santo N. Trehalose in desiccated rotifers: a comparison between a bdelloid and a monogonont species. Comp Biochem Physiol A Mol Integr Physiol. 2004;139:527–32.

Cesari M, Altiero T, Rebecchi L. Identification of the trehalose-6-phosphate synthase (tps) gene in desiccation tolerant and intolerant tardigrades. Ital J Zool. 2012;79:530–40.

Chandarlapaty S, Errede B. Ash1, a daughter cell-specific protein, is required for pseudohyphal growth of *Saccharomyces cerevisiae*. Mol Cell Biol. 1998;18:2884–91.

Crowe JH, Clegg JS. *Anhydrobiosis*. 1973.

Crowe JH, Crowe LM, Chapman D. Preservation of membranes in anhydrobiotic organisms: the role of trehalose. Science. 1984;223:701–3. https://doi.org/10.1126/science.223.4637.701

Crowe JH, Hoekstra FA, Crowe LM. Anhydrobiosis. Annu Rev Physiol. 1992;54:579–99.

Cuevas-Velazquez CL, Saab-Rincón G, Reyes JL, Covarrubias AA. The unstructured N-terminal region of *Arabidopsis* group 4 late embryogenesis abundant (LEA) proteins is required for folding and for chaperone-like activity under water deficit. J Biol Chem. 2016;291:10893–903.

Das RK, Pappu RV (2013) Conformations of intrinsically disordered proteins are influenced by linear sequence distributions of oppositely charged residues. Proc Natl Acad Sci U S A 110:13392–7. Available from: https://pubmed.ncbi.nlm.nih.gov/23901099/

Deber CM, Brodsky B, Rath A. Proline residues in proteins. eLS. John Wiley & Sons, Ltd: United Kingdom; 2010.

Dorone Y, Boeynaems S, Flores E, Jin B, Hateley S, Bossi F, et al. A prion-like protein regulator of seed germination undergoes hydration-dependent phase separation. Cell. 2021;184:4284–4298.e27.

Drozdetskiy A, Cole C, Procter J, Barton GJ (2015) JPred4: a protein secondary structure prediction server. Nucleic Acids Res 43:W389–W394. Available from: https://pubmed.ncbi.nlm.nih.gov/25883141/

Dure L, Greenway SC, Galau GA (1981) Developmental biochemistry of cottonseed embryogenesis and germination: changing messenger ribonucleic acid populations as shown by in vitro and in vivo protein synthesis. Biochemistry 20. Available from: https://pubmed.ncbi.nlm.nih.gov/7284317/

Eicher JE, Brom JA, Wang S, Sheiko SS, Atkin JM, Pielak GJ. Secondary structure and stability of a gel-forming tardigrade desiccation-tolerance protein. Protein Sci. 2022;31:e4495.

Eisenberg D, Weiss RM, Terwilliger TC. The helical hydrophobic moment: a measure of the amphiphilicity of a helix. Nature. 1982;299:371–4.

Emenecker R, Griffith D, Holehouse AS. Metapredict: a fast, accurate, and easy-to-use predictor of consensus disorder and structure. Biophys J. 2021;120:4312–9.

Erkut C, Penkov S, Khesbak H, Vorkel D, Verbavatz J, Fahmy K, et al. Trehalose renders the dauer larva of *Caenorhabditis elegans* resistant to extreme desiccation. Curr Biol. 2011;21:1331–6.

Fukuda Y, Inoue T. Crystal structure of secretory abundant heat soluble protein 4 from one of the toughest "water bears" micro-animals *Ramazzottius varieornatus*. Protein Sci. 2018;27:993–9.

Fukuda Y, Miura Y, Mizohata E, Inoue T (2017) Structural insights into a secretory abundant heat-soluble protein from an anhydrobiotic tardigrade, *Ramazzottius varieornatus*. FEBS Lett 591:2458–69. Available from: https://pubmed.ncbi.nlm.nih.gov/28703282/

Furuki T, Sakurai M (2014) Group 3 LEA protein model peptides protect liposomes during desiccation. Biochim Biophys Acta 1838:2757–66. Available from: https://pubmed.ncbi.nlm.nih.gov/25037007/

Garay-Arroyo A, Colmenero-Flores JM, Garciarrubio A, Covarrubias AA. Highly hydrophilic proteins in prokaryotes and eukaryotes are common during conditions of water deficit. J Biol Chem. 2000;275:5668–74.

Goyal K, Walton LJ, Tunnacliffe A. LEA proteins prevent protein aggregation due to water stress. Biochem J. 2005;388:151–7.

Habchi J, Tompa P, Longhi S, Uversky VN. Introducing protein intrinsic disorder. Chem Rev. 2014;114:6561–88.

Hand SC, Menze MA, Toner M, Boswell L, Moore D (2011) LEA proteins during water stress: not just for plants anymore. Annu Rev Physiol 73:115–34. Available from: https://pubmed.ncbi.nlm.nih.gov/21034219/

Hara Y, Shibahara R, Kondo K, Abe W, Kunieda T. Parallel evolution of trehalose production machinery in anhydrobiotic animals via recurrent gene loss and horizontal transfer. Open Biol. 2021;11:200413.

Hengherr S, Heyer AG, Köhler H-R, Schill RO. Trehalose and anhydrobiosis in tardigrades—evidence for divergence in responses to dehydration. FEBS J. 2008;275:281–8.

Hesgrove C, Boothby TC (2020) The biology of tardigrade disordered proteins in extreme stress tolerance. Cell Commun Signal 18:1–15. Available from: https://pubmed.ncbi.nlm.nih.gov/33148259/

Hesgrove CS, Nguyen KH, Biswas S, Childs CA, Shraddha KC, Medina BX, et al. Tardigrade CAHS proteins act as molecular Swiss Army knives to mediate desiccation tolerance through multiple mechanisms. bioRxiv. 2021;2021–2008: 2021–2008.

Hincha DK, Thalhammer A (2012) LEA proteins: IDPs with versatile functions in cellular dehydration tolerance. Biochem Soc Trans 40:1000–3. Available from: https://pubmed.ncbi.nlm.nih.gov/22988854/

Holehouse AS, Das RK, Ahad JN, Richardson MOG, Pappu RV. CIDER: resources to analyze sequence-ensemble relationships of intrinsically disordered proteins. Biophys J. 2017;112:16–21.

Jönsson I, Persson O. Trehalose in Three Species of Desiccation Tolerant Tardigrades The Open Zoology Journal. 2010;3:1–5.

Kikawada T, Nakahara Y, Kanamori Y, Iwata K, Watanabe M, McGee B, Tunnacliffe A, Okuda T (2006) Dehydration-induced expression of LEA proteins in an anhydrobiotic chironomid. Biochem Biophys Res Commun 348:56–61. Available from: https://pubmed.ncbi.nlm.nih.gov/16875677/

Koubaa S, Bremer A, Hincha DK, Brini F. Structural properties and enzyme stabilization function of the intrinsically disordered LEA_4 protein TdLEA3 from wheat. Sci Rep. 2019;9:3720.

Lapinski J, Tunnacliffe A. Anhydrobiosis without trehalose in bdelloid rotifers. FEBS Lett. 2003;553:387–90. https://doi.org/10.1016/s0014-5793(03)01062-7

LeBlanc BM, Hand SC. Target enzymes are stabilized by AfrLEA6 and a gain of α-helix coincides with protection by a group

3 LEA protein during incremental drying. Biochim Biophys Acta Proteins Proteomics. 2021;1869:140642.

Malki A, Teulon JM, Camacho-Zarco AR, Chen SW, Adamski W, Maurin D, Salvi N, Pellequer JL, Blackledge M (2022) Intrinsically disordered tardigrade proteins self-assemble into fibrous gels in response to environmental stress. Angew Chem Int Ed Engl 61:e202109961. Available from: https://pubmed.ncbi.nlm.nih.gov/34750927/

Martin EW, Holehouse AS, Peran I, Farag M, Incicco JJ, Bremer A, et al. Valence and patterning of aromatic residues determine the phase behavior of prion-like domains. Science. 2020;367:694–9.

Micsonai A, Wien F, Bulyáki É, Kun J, Moussong É, Lee Y-H, et al. BeStSel: a web server for accurate protein secondary structure prediction and fold recognition from the circular dichroism spectra. Nucleic Acids Res. 2018;46:W315–22.

Mirdita M, Schütze K, Moriwaki Y, Heo L, Ovchinnikov S, Steinegger M. ColabFold: making protein folding accessible to all. Nat Methods. 2022;19:679–82.

Miyazawa K, Itoh SG, Watanabe H, Uchihashi T, Yanaka S, Yagi-Utsumi M, Kato K, Arakawa K, Okumura H (2021) Tardigrade secretory-abundant heat-soluble protein has a flexible β-barrel structure in solution and keeps this structure in dehydration. J Phys Chem B 125:9145–54. Available from: https://pubmed.ncbi.nlm.nih.gov/34375104/

Miyazawa K, Itoh SG, Yoshida Y, Arakawa K, Okumura H (2022) Tardigrade secretory-abundant heat-soluble protein varies entrance propensity depending on the amino-acid sequence. J Phys Chem B 126:2361–8. Available from: https://pubmed.ncbi.nlm.nih.gov/35316056/

Mok YK, Kay CM, Kay LE, Forman-Kay J. NOE data demonstrating a compact unfolded state for an SH3 domain under non-denaturing conditions. J Mol Biol. 1999;289:619–38.

Nguyen K, Kc S, Gonzalez T, Tapia H, Boothby TC. Trehalose and tardigrade CAHS proteins work synergistically to promote desiccation tolerance. Commun Biol. 2022;5:1046.

Packebush MH, Sanchez-Martinez S, Biswas S, Kc S, Nguyen KH, Ramirez JF, et al. Natural and engineered mediators of desiccation tolerance stabilize human blood clotting factor VIII in a dry state. Sci Rep. 2023;13:1–16.

Pettersen EF, Goddard TD, Huang CC, Meng EC, Couch GS, Croll TI, et al. UCSF ChimeraX: structure visualization for researchers, educators, and developers. Protein Sci. 2021;30:70–82.

Piszkiewicz S, Gunn KH, Warmuth O, Propst A, Mehta A, Nguyen KH, et al. Protecting activity of desiccated enzymes. Protein Sci. 2019;28:941–51.

Roesgaard MA, Lundsgaard JE, Newcombe EA, Jacobsen NL, Pesce F, Tranchant EE, et al. Deciphering the alphabet of disorder—Glu and Asp act differently on local but not global properties. Biomolecules. 2022;12:1426.

Romero-Perez PS, Dorone Y, Flores E, Sukenik S, Boeynaems S. When phased without water: biophysics of cellular desiccation, from biomolecules to condensates. Chem Rev. 2023;123:9010–35. https://doi.org/10.1021/acs.chemrev.2c00659

Sallon S, Solowey E, Cohen Y, Korchinsky R, Egli M, Woodhatch I, et al. Germination, genetics, and growth of an ancient date seed. Science. 2008;320:1464.

Sanchez-Martinez S, Nguyen K, Biswas S, Nicholson V, Romanyuk AV, Ramirez JF, et al. Labile assembly of a tardigrade protein induces biostasis. bioRxiv. 2023;2023.06.30.547219. https://doi.org/10.1101/2023.06.30.547219v1.abstract

Sanchez-Martinez S, Ramirez JF, Meese EK, Childs CA, Boothby TC. The tardigrade protein CAHS D interacts with, but does not retain, water in hydrated and desiccated systems. Sci Rep. 2023;13:10449.

Schokraie E, Hotz-Wagenblatt A, Warnken U, Mali B, Frohme M, Förster F, Dandekar T, Hengherr S, Schill RO, Schnölzer M (2010) Proteomic analysis of tardigrades: towards a better understanding of molecular mechanisms by anhydrobiotic organisms. PLoS One 5:e9502. Available from: https://www.ncbi.nlm.nih.gov/pmc/articles/PMC2835947/

Shimizu T, Kanamori Y, Furuki T, Kikawada T, Okuda T, Takahashi T, Mihara H, Sakurai M (2010) Desiccation-induced structuralization and glass formation of group 3 late embryogenesis abundant protein model peptides. Biochemistry 49:1093–104. Available from: https://pubmed.ncbi.nlm.nih.gov/20028138/

Shou K, Bremer A, Rindfleisch T, Knox-Brown P, Hirai M, Rekas A, et al. Conformational selection of the intrinsically disordered plant stress protein COR15A in response to solution osmolarity—an X-ray and light scattering study. Phys Chem Chem Phys. 2019;21:18727–40.

Sowemimo OT, Knox-Brown P, Borcherds W, Rindfleisch T, Thalhammer A, Daughdrill GW. Conserved glycines control disorder and function in the cold-regulated protein, COR15A. Biomolecules. 2019;9:84. https://doi.org/10.3390/biom9030084

Tanaka A, Nakano T, Watanabe K, Masuda K, Honda G, Kamata S, et al. Stress-dependent cell stiffening by tardigrade tolerance proteins that reversibly form a filamentous network and gel. PLoS Biol. 2022;20:e3001780.

Tanaka S, Tanaka J, Miwa Y, Horikawa DD, Katayama T, Arakawa K, et al. Novel mitochondria-targeted heat-soluble proteins identified in the anhydrobiotic tardigrade improve osmotic tolerance of human cells. PLoS One. 2015;10:e0118272.

Tapia H, Koshland DE. Trehalose is a versatile and long-lived chaperone for desiccation tolerance. Curr Biol. 2014;24:2758–66.

Tolleter D, Hincha DK, Macherel D. A mitochondrial late embryogenesis abundant protein stabilizes model membranes in the dry state. Biochim Biophys Acta Biomembr. 2010;1798:1926–33.

Tunnacliffe A, Hincha DK, Leprince O. Macherel D LEA proteins: versatility of form and function. In: Lubzens E, Cerda J, Clark M, editors. Dormancy and resistance in harsh environments. Berlin, Heidelberg: Springer Berlin Heidelberg; 2010. p. 91–108.

Tunnacliffe A, Lapinski J. Resurrecting Van Leeuwenhoek's rotifers: a reappraisal of the role of disaccharides in anhydrobiosis. Philos Trans R Soc Lond Ser B Biol Sci. 2003;358:1755–71.

Tunnacliffe A, Lapinski J, McGee B. A putative LEA protein, but no trehalose, is present in anhydrobiotic bdelloid rotifers. Hydrobiologia. 2005;546:315–21.

Tunnacliffe A, Wise MJ. The continuing conundrum of the LEA proteins. Naturwissenschaften. 2007;94:791–812.

Walker JM. The proteomics protocols handbook. Springer Science & Business Media: New Jersey; 2007.

Wang S, Eicher J, Pielak GJ. Trifluoroethanol and the behavior of a tardigrade desiccation-tolerance protein. Protein Sci. 2023;32:e4716.

Westh P, Ramløv H. Trehalose accumulation in the tardigrade *Adorybiotus coronifer* during anhydrobiosis. J Exp Zool. 1991; 258:303–11. https://doi.org/10.1002/jez.1402580305

Woolfson DN, Williams DH. The influence of proline residues on α-helical structure. FEBS Lett. 1990;277:185–8.

Yagi-Utsumi M, Aoki K, Watanabe H, Song C, Nishimura S, Satoh T, et al. Desiccation-induced fibrous condensation of CAHS protein from an anhydrobiotic tardigrade. Sci Rep. 2021;11:1–9.

Yamaguchi A, Tanaka S, Yamaguchi S, Kuwahara H, Takamura C, Imajoh-Ohmi S, et al. Two novel heat-soluble protein families abundantly expressed in an anhydrobiotic tardigrade. PLoS One. 2012;7:e44209.

SUPPORTING INFORMATION

Additional supporting information can be found online in the Supporting Information section at the end of this article.

How to cite this article: Biswas S, Gollub E, Yu F, Ginell G, Holehouse A, Sukenik S, et al. Helicity of a tardigrade disordered protein contributes to its protective function during desiccation. Protein Science. 2024;33(2):e4872. https://doi.org/10.1002/pro.4872